Nat. Hazards Earth Syst. Sci. Discuss., 1, 5729–5752, 2013
www.nat-hazards-earth-syst-sci-discuss.net/1/5729/2013/
doi:10.5194/nhessd-1-5729-2013

Natural Hazards and Earth System Sciences Discussions
Open Access

Combining earthquakes and GPS data to estimate the probability of future earthquakes with magnitude $M_w \geq 6.0$

K.-P. Chen[1], **Y.-B. Tsai**[2], **and W.-Y. Chang**[3]

[1]Hsin Sheng Junior College of Medical Care and Management, No. 418, Gaoping Sec., Jhongfong Rd., Longtan, Taoyuan County 32544, Taiwan
[2]Geosciences Department, Pacific Gas and Electric Company, One Market, Spear Tower, Suite 2400 San Francisco, CA 94105-1126, USA
[3]Department of Natural Resources and Environmental Studies, NDHU, No. 1, Sec. 2, Da Hsueh Rd., Shoufeng, Hualien 97401, R.O.C., Taiwan

Received: 24 May 2013 – Accepted: 6 September 2013 – Published: 22 October 2013

Correspondence to: K.-P. Chen (chenkueipao@yahoo.com.tw)

Published by Copernicus Publications on behalf of the European Geosciences Union.

Abstract

According to Wyss et al. (2000) result indicates that future main earthquakes can be expected along zones characterized by low *b* values. In this study we combine Benioff strain with global positioning system (GPS) data to estimate the probability of future $M_w \geq 6.0$ earthquakes for a grid covering Taiwan. An approach similar to the maximum likelihood method was used to estimate Gutenberg–Richter parameters *a* and *b*. The two parameters were then used to estimate the probability of simulating future earthquakes of $M_w \geq 6.0$ for each of the 391 grids (grid interval = 0.1°) covering Taiwan. The method shows a high probability of earthquakes in western Taiwan along a zone that extends from Taichung southward to Nantou, Chiayi, Tainan and Kaohsiung. In eastern Taiwan, there also exists a high probability zone from Ilan southward to Hualian and Taitung. These zones are characterized by high earthquake entropy, high maximum shear strain rates, and paths of low *b* values. A relation between entropy and maximum shear strain rate is also obtained. It indicates that the maximum shear strain rate is about 4.0 times the entropy. The results of this study should be of interest to city planners, especially those concerned with earthquake preparedness. And providing the earthquake insurers to draw up the basic premium.

1 Introduction

In any given region, the Gutenberg–Richter (1944) equation describes the relationship between magnitude and the total number of earthquakes of at least that magnitude: $\log_{10}(N) = a - bM$, where N is the number of earthquake with magnitude equal to or greater than M; a is proportional to the seismicity rate; and b describes the size distribution of events. The a and b parameters characterize temporal and quantitative earthquake seismicity, respectively. Estimation of the two parameters can be derived from a number of statistical processes. Some authors specify the physical meanings of each parameter. For example, Aki (1965) suggested a relationship between b

NHESSD

1, 5729–5752, 2013

and fault fractal dimension, D. This was later confirmed by Turcotte (1997) with the relationship expressed as $D = 2b$. Hirata (1989), however, provided an alternative empirical relationship of $D = \alpha - \beta b$, where $\alpha = 1.8 - 2.3$ and $\beta = 0.56 - 0.73$. More recent studies by Singh et al. (2008, 2009) have shown that there is not a simple relationship between D and b values. They contend the relationship changes according to stress distribution. Furthermore, Schorlemmer et al. (2005) proposed b values acting as inverse stress meters because they depend inversely on differential stress. Some researchers (Aki, 1965; Utsu, 1965) have attempted to give further insight into the Guternberg–Richer Law based on maximum likelihood estimations. Aki (1965), in particular, used the maximum likelihood method to estimate b value and its statistical error.

Entropy is a fundamental physical and statistical quantity that characterizes the complexity of the dynamic nature of a physical process (Ben-Naim, 2008). Entropy is the quantitative measure of disorder in a system. The concept comes out of thermodynamics, which deals with the transfer of heat energy within a system. In an isothermal process, the change in entropy (δS) is the change in heat (Q) divided by the absolute temperature (T): $\delta S = Q/T$. In any reversible thermodynamic process (when there is some sort of energetic change within the system, generally associated with changes in pressure, volume, internal energy, temperature, or any sort of heat transfer) it can be represented in calculus as the integral from a processes initial state to final state of dQ/T. Shannon (1948) applied the entropy concept to information theory to describe the properties of long sequences of symbols when transmitting or receiving messages. Nicholson et al. (2000) introduced spatial entropy to quantify the simplification of earthquake distributions due to relocation processes while Telesca et al. (2004) applied the temporal definition of entropy to the Umbria-Marche 1997 seismic sequence. Other researchers (Main and Burton, 1984) maximized Shannon entropy to find a new frequency–magnitude relation consistent with the averages of magnitude M and seismic moment.

In this study, Shannon entropy is applied to the historical catalog of Taiwan's earthquakes as described by Chen et al. (2010). We combine Benioff strain with global positioning system (GPS) data to estimate the probability of future $M_w \geq 6.0$ earthquakes on a grid for Taiwan. Maximum likelihood estimation is used based on the Gutenberg–Richter relationship to estimate earthquake entropy and associated a and b values, because the earthquake entropy is relevant to b. The results of this approach show that high earthquake entropy correlates with zones where the rate of maximum shear strain is also high. Additionally, the b value is inversely related to the maximum shear strain rate. Next, the estimated a and b values are used to simulate the probability of future earthquakes of magnitude $M_w \geq 6.0$ for a network of 391 grid points (grid interval = 0.1°) covering Taiwan. Results show that in western Taiwan, a high probability extends along a zone from Hsinchu southward to Taichung, Nantou, Chiayi, Tainan, and Kaohsiung while in eastern Taiwan, a similar phenomenon occurs from Ilan southward to Hualian and Taitung. These paths also have maximum shear strain rate, and low b values. Low b values are indicative of future mainshocks (Lockner and Byerlee, 1991; Wyss et al., 2000). These estimates should be of interest to city planners, especially those concerned with earthquake preparedness.

2 Probability of earthquakes and estimates of *a* and *b* values in the Gutenberg–Richter law

The Gutenberg–Richter relationship $\log n(M) = a - bM$ is an expression involving the cumulative estimate of magnitude M's probability density function $p(M)$ whereby:

$$p(M) = b \times 10^{-b(M-M_{0L})}/\log_{10}e \quad (1)$$

M_{0L} is the minimum magnitude for which the seismic catalog is complete. Let us consider the mean value of all possible magnitudes ($\overline{M}$) in a given time interval (T)

NHESSD
1, 5729–5752, 2013

over which M is defined as:

$$\overline{M} = \int\limits_{M_{0L}}^{\infty} mp(m)\mathrm{d}m. \tag{2}$$

Inserting the expression $p(M)$ into Eq. (2), we get:

$$\overline{M} = \int\limits_{M_{0L}}^{\infty} mp(m)\mathrm{d}m = \frac{b \times 10^{bM_{0L}}}{\log_{10} e} \int\limits_{M_{0L}}^{\infty} m \times 10^{-bm}\mathrm{d}m. \tag{3}$$

The latter integral can be solved by partial integration giving:

$$\overline{M} = M_{0L} + \frac{\log_{10} e}{b}. \tag{4}$$

Rearranging terms we get:

$$b = \frac{\log_{10} e}{\left(\overline{M} - M_{0L}\right)}. \tag{5}$$

The expression is the same as given by Aki (1965). There is also an expression for the a value:

$$a = \log_{10}(N/T) + b\,M_{0L}. \tag{6}$$

The Shannon entropy H is defined as (Shannon, 1948)

$$H(t) = -\sum_{i=1}^{K} p_i(t)\,\log_{10} p_i(t) \tag{7}$$

NHESSD
1, 5729–5752, 2013

Probability of future earthquakes with $M_w \geq 6.0$

K.-P. Chen et al.

where K is the number of classes of events, $p_i(t)$ is the probability of occurrence in each i-th class (when $p_i = 0$, $p_i \log p_i = 0$). If probability is a continuous function whereby magnitude probability $p = p(M,t)$, and Shannon entropy is rewritten as an integral (Wiener, 1948)

$$H(t) = -\int_{M_o}^{\infty} p(M,t)\log_{10} p(M,t)\mathrm{d}M \tag{8}$$

for a certain time t, then taking into account the expression of probability Eq. (1) and the b value Eq. (5), we obtain entropy whereby:

$$H(t) = \log_{10}(e\log_{10}e) - \log_{10}b = k' - \log_{10}b \tag{9}$$

where $k' = \log_{10}(e\log_{10}e) \approx 0.072$. After re-arranging of Eq. (9) an alternate expression is to simply write the relationship between entropy and b value as:

$$b = \frac{b_{\max}}{10^H} \approx \frac{1.2}{10^H} \tag{10}$$

where $b_{\max} = e\log_{10}e \approx 1.2$

Finally, because Eq. (5) expresses the relation between b and $\overline{M}$, we can express entropy as:

$$H(t) = \log_{10}e + \log_{10}(\overline{M} - M_{0\mathrm{L}}) \tag{11}$$

3 Data processing and interpretation

Taiwan is located at the juncture of the Philippine Sea plate and Eurasian plate. Earthquakes occur very frequently as shown in Fig. 1. Taiwan has a relatively complete earthquake catalog $M_w \geq 2.0$, dating back to the installation of the first seismograph in 1897. Data used in this study is based on Chen and Tsai's (2008) study that converted the original magnitudes of Taiwan's earthquake catalog 1900–2006 into homogenized M_w magnitudes. The catalog has since been updated to include earthquakes up to 2008, and supplementary data found in the literature for the time period 1900–1935 (Chen et al., 2010) for a complete catalog of $M_w \geq 5.0$ earthquakes. There are 1989 $M_w \geq 5.0$ crustal earthquakes. We then use these data to match with a relative attenuation law to create peak ground acceleration (PGA) and peak ground velocity (PGV) for each of 391 grid points (grid interval is 0.1°). We further combined the PGA and PGV values to obtain corresponding Modified Mercalli intensity (MMI) values (Wald et al., 1999), the result shown in Fig. 2. Following, we adopted a logarithmic functional form analogous to the Gutenberg–Richter relation for seismicity to represent the annual frequency of seismic intensity parameters: $\log_{10}(N) = a - b\log_{10}(\mathrm{PGA})$, $\log_{10}(N) = a - b\log_{10}(\mathrm{PGV})$, and $\log_{10}(N) = a - bI$. It is found that the regions with high rate of exceeding particular PGA, PGV and MMI values are often associated with low b values in these equations as shown in Fig. 3. Figure 3 shows the spatial distributions of a and b for PGA, PGV and MMI for the whole of Taiwan. It is evident that low b values in western Taiwan extend along a zone from Taichung southward to Nantou, Chiayi, Tainan and Kaohsiung. In eastern Taiwan, there also exists a low b values zone from Ilan southward to Hualian and Taitung. This pattern suggests that these areas can expect future strong shaking (Lockner and Byerlee, 1991). The a values of PGA and MMI have similar trends, but they are somewhat different for PGV, probably due to difference between the attenuation relationships for PGA and PGV.

To conduct the study, Taiwan Island is divided into 391 grid points at a grid interval of 0.1°. To ensure a complete dataset and increase data volume for better confidence in the Gutenberg–Richter frequency-magnitude distribution, earthquakes of magnitude as low as $M_w \geq 1.0$ were selected to calculate earthquake entropy at each grid. Firstly, data from each grid point were plotted on a cumulative frequency-magnitude distribution. Second, the linear section of the relationship was selected to obtain

NHESSD
1, 5729–5752, 2013

minimum magnitude M_{0L} and M_i with respect to number n_i, allowing for the calculation of average magnitude $\overline{M}$

$$\overline{M} = \sum_{i=1}^{N} \frac{n_i M_i}{n_i}, \tag{12}$$

where N is the number of classes of magnitude. Next, earthquake entropy of each grid point was calculated as per Eq. (11) (Fig. 4a). b values were calculated as per Eq. (10) (Fig. 4b). Figure 4a shows high entropy along a zone extending from Taichung southward to Nantou, Chiayi, Tainan, and Kaohsiung in western Taiwan and from Ilan southward to Hualian and Taitung in eastern Taiwan. These zones are also low b value paths (Fig. 4b) by definition (Eq. 10). GPS data (Hsu et al., 2008) was used to calculate the maximum shear strain rate similar to Hsu et al. (2009) as shown in Fig. 4c. Figure 4a and c show the relationship between earthquake entropy and maximum shear strain rates. From these figures, the trend in high entropy is similar to the trend in maximum shear strain rate. For all grid points that each grid has its own earthquake entropy and maximum shear strain rate, and we use the least square fit to determine the coefficients of the linear fit, and the result is shown as Fig. 5. Figure 5 shows the quantitative relationship between entropy and maximum shear strain rate. Note that maximum shear strain rate is about 4.0 times the standard deviation of earthquake entropy.

4 Forecasting the probability of future earthquakes of $M_w \geq 6.0$

The crustal strain rate tensor provides a description of geodynamic processes such as fault strain accumulation, which is an important parameter for seismic hazard assessment (Hackl et al., 2009). Assuming small deformations, the components of the strain rate tensor are defined as:

$$\varepsilon_{ij} = \frac{1}{2}\left(\frac{\partial v_i}{\partial x_j} + \frac{\partial v_j}{\partial x_i}\right), \quad (13)$$

where i and j substitute for east and north, respectively.

In a similar way, it is possible to compute the antisymmetric rotation rate tensor:

$$\omega_{ij} = \frac{1}{2}\left(\frac{\partial v_i}{\partial x_j} - \frac{\partial v_j}{\partial x_i}\right). \quad (14)$$

At this point, any tensorial analysis can be performed.

The eigenvector of the strain rate represents the direction of maximum and minimum strain rates, while their associated real eigenvalues λ_1 and λ_2 represent the magnitude (i.e. positive values indicate extension and negative values compression). The maximum shear strain rate at every grid point can be obtained by a linear combination of the maximum and minimum eigenvalues:

$$\varepsilon_{\text{max\_shear}} = \frac{\lambda_1 - \lambda_2}{2}. \quad (15)$$

During data processing calculation of the maximum shear strain rate may cause uncertainty. The source of this uncertainty comes from observed data. It is transferred to the velocity field and ultimately the shear strain rate; i.e., uncertainty is cumulative. In this study, the shear strain average uncertainty is 0.113 ± 0.0146.

Assuming probability is an appropriate approach to earthquake prediction, the probability of a $M_w \geq 6.0$ earthquake occurring at each grid point in the future is estimated. Shen et al. (2007) had combined the earthquakes data with GPS data, but their formulas is very complex, and the result is not good. Therefore, I try to find new method, the method combines Benioff strain with maximum shear strain rate. Although, my method is naïve, but it is easy and convenient, The annual probability

NHESSD
1, 5729–5752, 2013

of an earthquake at a given location x, given a Benioff strain for each grid point is described by:

$$P(x,\overline{B}) = A(x)\overline{B}, \tag{16}$$

where $A(x)$ is the maximum shear strain rate field, and

$$\overline{B} = \frac{B_{xy} - B_{\min}}{B - B_{\min}}. \tag{17}$$

Cumulative Benioff strain is defined as:

$$B_{xy} = \sum_{i=1}^{N} \sqrt{E_{xy}^{(i)}}, \tag{18}$$

where $E_{xy}^{(i)}$ is the seismic energy release in the i-th earthquake, N is the number of earthquakes considered at each grid point, and xy is the coordinates of a given grid point. The seismic energy E is related to the seismic moment M_0. $B_{\min}$ is the Benioff strain of minimum magnitude of each grid point, B is the Benioff strain at each grid for future earthquakes of magnitude $\geq M$, it is Eq. (18) with $N = 1$ and E corresponding to a $M = 6$ earthquake. Maximum shear strain rate is estimated by GPS data (Hsu et al., 2009) and the interpolated strain rate is assigned to each grid point (Fig. 4c); the results of the annual probability of $M = 6$ are shown in Fig. 6. Here, it is evident that high probability zones exist along zones extending from Taichung southward to Nantou, Chiayi, Tainan and Kaohsiung in western Taiwan and from Ilan southward to Hualian and Taitung in eastern Taiwan. Along fault zones, anomalously low b values map asperities (Wiemer and Wyss, 1997; Wyss, 2001). A corollary of the latter observation is that the rupture initiation points of mainshocks may be mapped by low b value volumes (Wyss et al., 2000). Therefore, the high probability zones are also low b value paths, indicating potential future mainshocks.

5 Simulating future earthquakes

According to Gutenberg–Richter (1944) earthquake frequency-magnitude distribution, we can re-write it as:

$$N = 10^{a-bM}. \tag{19}$$

If the occurrence of an earthquake is a random process (Poisson process), then the probability of at least one earthquake of magnitude $\geq M$ within one year is:

$$p_1 = 1 - e^{-N} = 1 - e^{-10^{a-bM}} = 1 - e^{-e^{\ln 10^{a-bM}}}. \tag{20}$$

After derivation:

$$M = \frac{a}{b} - \frac{1}{b\ln 10}\ln(-\ln(1-p_1)), \tag{21}$$

where p_1 is a random number picked from a uniform distribution over the closed interval (0, 1).

And the time from a random event generator can be derived (Bury, 1999) as:

$$t = -10^{-a}\ln(v), \tag{22}$$

where t is a random time interval between events, v is a random number picked from a uniform distribution over the closed interval (0, 1).

Therefore, the probability of at least one earthquake of magnitude $\geq M$ within t years is:

$$p = 1 - e^{-Nt} = 1 - e^{-(10^{a-bM})\,t}. \tag{23}$$

Therefore, we can use Eqs. (21)–(23), and a, b calculated from Eqs. (6) and (10) to simulate the magnitudes, probabilities, and times of future earthquakes (Fig. 7). To

NHESSD
1, 5729–5752, 2013

recognize any trends in the probability of future earthquakes of $M_w \geq 6.0$ for each grid point, the probabilities of such earthquakes occurring within the next 10, 20, 30, and 50 yr at each grid point are shown in Fig. 8. From Fig. 8, there are high probability zones extending from Taichung southward to Nantou, Chiayi, Tainan and Kaohsiung in western Taiwan and from Ilan southward to Hualian and Taitung in eastern Taiwan. Equation (16) is to combine the maximum shear strain rate and Benioff strain to estimate the probability of future earthquake $M_w = 6.0$ of each grid point, but, Eq. (23) is to simulate the probability trend of future earthquake $M_w \geq 6.0$ of each grid point. Therefore, the result of simulating can verify the previous results.

6 Conclusions

In this study, there are 1989 $M_w \geq 5.0$ crustal earthquakes. We then use these data to match with a relative attenuation law to create peak ground acceleration (PGA) and peak ground velocity (PGV) for each of 391 grid points (grid interval is 0.1°). We further combined the PGA and PGV values to obtain corresponding Modified Mercalli intensity (MMI) values (Wald et al., 1999). b value is an important parameter for seismic hazard assessment. It is from $\log_{10}(N) = a - b\log_{10}(\mathrm{PGA})$, $\log_{10}(N) = a - b\log_{10}(\mathrm{PGV})$, and $\log_{10}(N) = a - bI$ to estimate a, b values respectively. It is found that the regions with high PGA, PGV and MMI values are often associated with low b values for a, b from the PGA, PGV, and MMI relations. The low b values paths Taichung southward to Nantou, Chiayi, Tainan, and Kaohsiung in western Taiwan, and from Ilan southward to Hualien and Taitung in eastern Taiwan. Earthquake entropy is a parameter related to b values. In this study, data from the cumulative frequency–magnitude relationship for each of 391 grid points (at an interval of 0.1°) covering Taiwan was average magnitudeand earthquake entropy. Sequentially, b and a values for each grid point were obtained. After comparing b values and maximum shear strain rate, it is obvious b values are inversely related to the maximum shear strain rate. Evidently, the maximum shear strain rate is about 4.0 times the standard deviation of the entropy.

NHESSD
1, 5729–5752, 2013

Combining the Benioff strain and maximum shear strain rate, the annual probability of future earthquakes of magnitude $M_w \geq 6.0$ was estimated for each grid point. A high probability of future earthquakes exists for two separate regions of Taiwan. One is a zone that stretches from Hsinchu southward to Taichung, Nantou, Chiayi, Tainan, and Kaohsiung in western Taiwan, and the other from Ilan southward to Hualian and Taitung in eastern Taiwan. Projections out to 50 yr verify these zones as having high earthquake probabilities for $M_w \geq 6.0$ earthquakes. These zones are characterized by high maximum PGA, PGV, and MMI, high entropy, high maximum shear strain rates, and low *b* values. Low *b* values are indicative of future mainshocks (Wyss et al., 2000).

In some aspects, we must to remove foreshocks and aftershocks, but in this study for increasing data volume and confidence of each grid point, we do not remove foreshocks and aftershocks. Because, in this study we calculate the average magnitude is based on Gutenberg–Richter distribution, we then select linear section to calculate the average magnitude, then estimating the earthquake entropy, finally estimating the associated *a*, *b* values. If removing foreshocks and aftershocks that reduce the data volume of each grid point, and lead to reduce the average magnitude and earthquake entropy, hence increase *b* value, but reduces *a* value, and some grids do not have any earthquake data would be given up. And we want to understand the relation between the total seismic energy release by all earthquakes within each grid point with maximum shear strain rate. If removing foreshocks and aftershocks, we could not get the total seismic energy release of each grid, and some grids do not have any earthquake data would be given up. Because from Fig. 1, we can see some regions less often to occur earthquakes than surrounding, but the crustal deformation is large (Fig. 4c), especially in the south-western Taiwan. Therefore, In this study we combine the maximum shear strain rate with Benioff strain to estimate the probability of future earthquake $M_w \geq 6.0$. If removing foreshocks and aftershocks will reduce the estimated probability of future earthquake $M_w \geq 6.0$

NHESSD
1, 5729–5752, 2013

7 Data and resources

All data sources are taken from published works listed in the References. Some plots were made using the Generic Mapping Tools version 4.3.1 (www.soest.hawaii.edu/gmt; Wessel and Smith, 1998, last access: August 2006).

Acknowledgements. This study is supported by NSC 99-2116-M-570-001.

References

Aki, K.: Maximum likelihood estimate of b in the formula $\log(N) = a - bM$ and its confidence limits, Bull. Earthq. Res. Inst. Tokyo Univ., 43, 237–239, 1965.

Ben-Naim, A.: A farewell of entropy: statistical thermodynamics based on information, World Scientific, New Jersey, 2008.

Bury, K.: Statistical Distributions in Engineering, Cambridge University Press, Cambridge, ISBN 0 521 63506 3, 1999.

Chen, K. P. and Tsai, Y. B.: A catalog of Taiwan earthquakes (1900–2006) with homogenized M_W magnitudes, B. Seismol. Soc. Am., 98, 483–489, 2008.

Chen, K. P., Tsai, Y. B., Cheng, C. T., Liu, K. S., and Chang, W. Y.: Estimated seismic intensity distributions for earthquakes in Taiwan from 1900 to 2008, B. Seismol. Soc. Am., 100, 2905–2913, doi:10.1785/0120090397, 2010.

Gutenberg, B. and Richter, F.: Frequency of earthquakes in California, B. Seismol. Soc. Am., 34, 185–188, 1944.

Hackl, M., Malservisi, R., and Wdowinski, S.: Strain rate patterns from dense GPS networks, Nat. Hazards Earth Syst. Sci., 9, 1177–1187, doi:10.5194/nhess-9-1177-2009, 2009.

Hirata, T.: A correlation between the b value and the fractal dimension of earthquakes, J. Geophys. Res., 94, 7507–9514, 1989.

Hsu, Y. J., Yu, S. B., Simons, M., Kuo, L. C., and Chen, H. Y.: Interseismic crustal deformation in the Taiwan plate boundary zone revealed by GPS observations, seismicity, and earthquake focal mechanisms, Tectonophysics, 479, 4–18, 2009.

Lockner, D. A. and Byerlee, J. D.: Precursory AE patterns leading to rock fracture, in: Proc. 5th Conf. on AE/Microseismic activity in Geologic Structures and Materials, 45–58, edited by:

Hardy, H.R., Trans-Tech Publications Clausthal Zellerfeld and Pennsylvania State University, 1991.
Main, I. and Burton, P. W.: Information theory and the earthquake frequency-magnitude distribution, B. Seismol. Soc. Am., 74, 1409–1426, 1984.
Nicholson, T., Sambridge, M., and Gudmundsson, O.: On entropy and clustering in earthquake hypocenter distributions, Geophys. J. Int., 142, 37–51, 2000.
Schorlemmer, D., Wiemer, S., and Wyss, M.: Variation in earthquake size distribution across different stress regimes, Nature 437, 539–542, 2005.
Shannon, C. E.: A mathematical theory of communication, Bull. Syst. Tech. J., 27, 379–423, 623–656, 1948.
Shen, Z. K., Jackson, D. D., and Kagan, Y. Y.: Implication of geodetic strain rate for future earthquakes, with a five-year forecast of M5 earthquakes in Southern California, Seismol. Res. Lett., 78, 116–120, 2007.
Singh, C., Bhattacharya, P. M., and Chadha, R. K.: Seismicity in the Konya-Wama reservoir site in western India: fractal and *b* value mapping, B. Seismol. Soc. Am., 98, 476–482, 2008.
Singh, C., Singh, A., and Chadha, R. K.: Fractal and *b* value in eastern Himalaya and southern Tibet, B. Seismol. Soc. Am., 99, 3529–3533, 2009.
Telesca, L., Lapenna, V., and Lovallo, M.: Information entropy analysis of seismicity of Umbria-Marche region (Central Italy), Nat. Hazards Earth Syst. Sci., 4, 691–695, doi:10.5194/nhess-4-691-2004, 2004.
Turcotte, R.: Fractals and Chaos in Geology and Geophysics, Cambridge University Press, Cambridge, 1997.
Utsu, T.: A method for determining the value of *b* in a formula $\log n = q - bM$ showing the magnitude–frequency relation for earthquake, Proc. Microzonation Conf., Seattle, Washington, 897–909, 1965.
Wald, D. J., Quitoriano, V., Heaton, T. H., Kanamori, H., Scrivner, C. W., and Worden, C. B.: Trinet "ShakeMaps": rapid generation of peak ground motion and intensity maps for earthquakes in southern California, Earthq. Spectra, 15, 537–555, 1999.
Wiener, N.: Cybernetics, MIT Press, Cambridge, Massachussets, 1948.
Wessel, P. and Smith, W. H. F.: New, improved version of generic mapping tools released, EOS T. Am. Geophys. Un., 79, 579–579, doi:10.1029/98EO00426, 1998.

NHESSD
1, 5729–5752, 2013

Probability of future earthquakes with $M_w \geq 6.0$

K.-P. Chen et al.

Wiemer, S. and Wyss, M.: Mapping the frequency-magnitude distribution in asperities: an improved technique to calculate recurrence times?, J. Geophys. Res., 102, 15115–15128, 1997.

Wyss, M., Schorlemmer, D., and Wiemer, S.: Mapping asperities by minima of local recurrence time: the San Jacinto–Elsinore fault zones, J. Geophys. Res., 105, 7829–7844, 2000.

NHESSD

1, 5729–5752, 2013

Probability of future earthquakes with $M_w \geq 6.0$

K.-P. Chen et al.

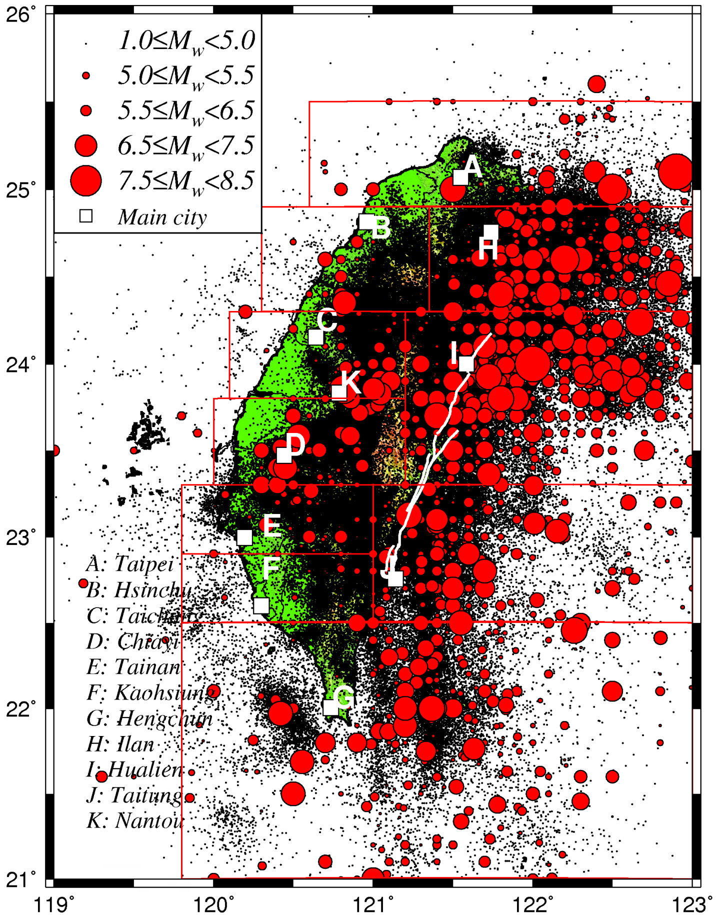

Fig. 1. The epicenter distributions of earthquakes from 1900 to 2008. The white curve line is the juncture of the Philippine Sea plate and Eurasian plate.

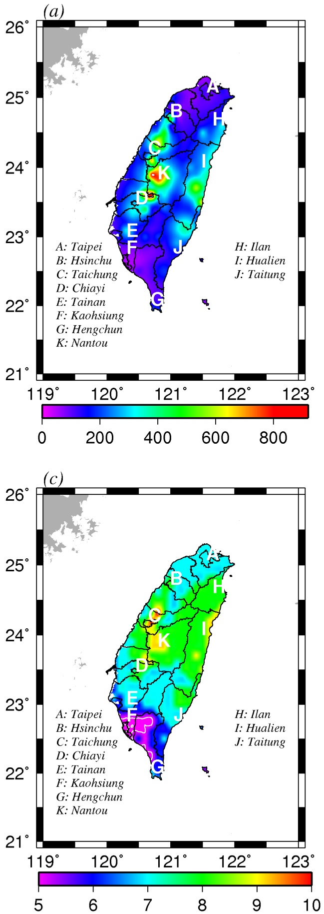

Fig. 2. Contour of estimated maximum PGA, maximum PGV and maximum MMI for earthquakes in Taiwan during 1900 to 2008. **(a)** Maximum PGA, **(b)** Maximum PGV, and **(c)** Maximum MMI.

NHESSD
1, 5729–5752, 2013

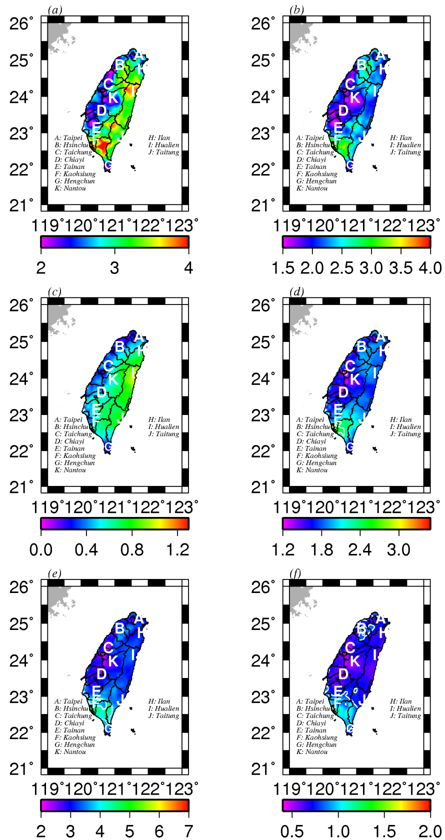

Fig. 3. The contour of respective *a*, *b* values for PGA, PGV, and MMI. Areas of low *b* values tend to coincide with areas of high PGA and PGV values. **(a)** *a* values of PGA, **(b)** *b* values of PGA, **(c)** *a* values of PGV, **(d)** *b* values of PGV, **(e)** *a* values of MMI, and **(f)** *b* values of MMI.

NHESSD
1, 5729–5752, 2013

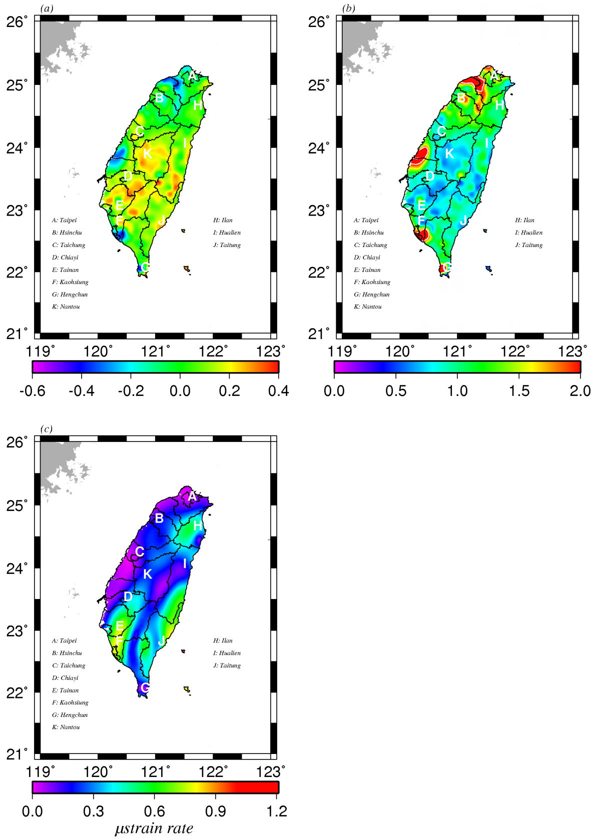

Fig. 4. **(a)** The entropy of earthquakes at each grid point for Taiwan. High entropy zones are from Taichung southward to Nantou, Chiayi, Tainan and Kaohsiung in western Taiwan and from Ilan southward to Hualian and Taitung in eastern Taiwan. **(b)** The *b* value distribution of each grid with respect to **(a)**. The low *b* value trend is the same as the trend in high entropy. **(c)** The distribution of maximum shear strain rate at each grid point for Taiwan. The high maximum shear strain rate trend is the same as the trend in high entropy.

NHESSD
1, 5729–5752, 2013

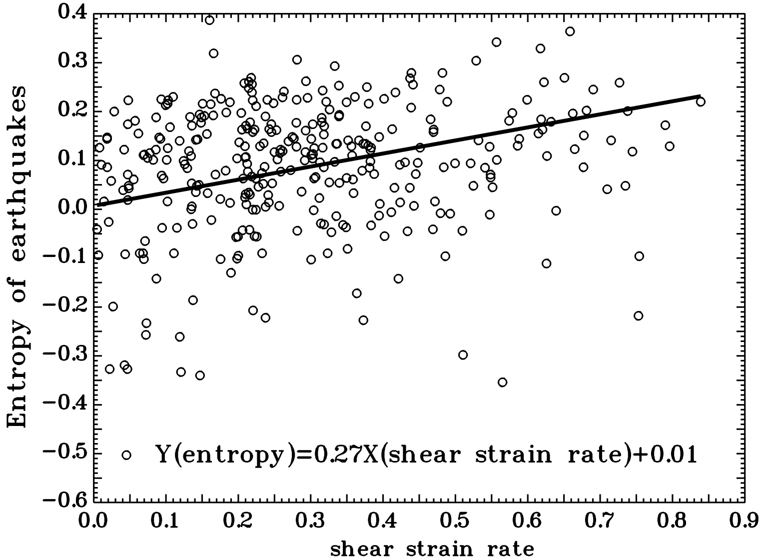

Fig. 5. The relation between entropy of earthquakes and maximum shear strain rate. Maximum shear strain rate is about 4.0 times entropy.

NHESSD

1, 5729–5752, 2013

Probability of future earthquakes with $M_w \geq 6.0$

K.-P. Chen et al.

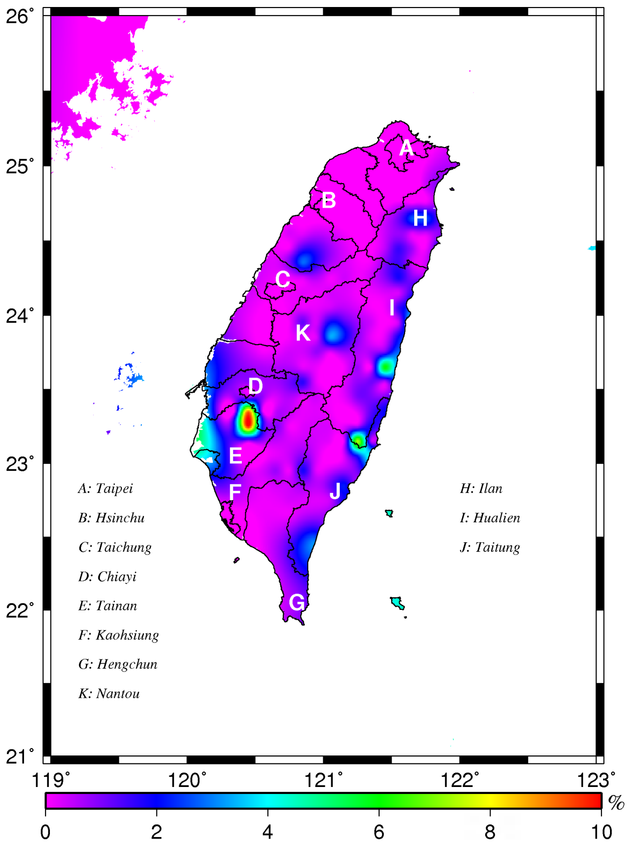

Fig. 6. Combining the Benioff strain and maximum shear strain rate to forecast the annual probability of future earthquakes of $M_w \geq 6.0$. High probability exists from Taichung southward to Nantou, Chiayi, Tainan, and Kaohsiung in western Taiwan and from Ilan southward to Hualian and Taitung in eastern Taiwan.

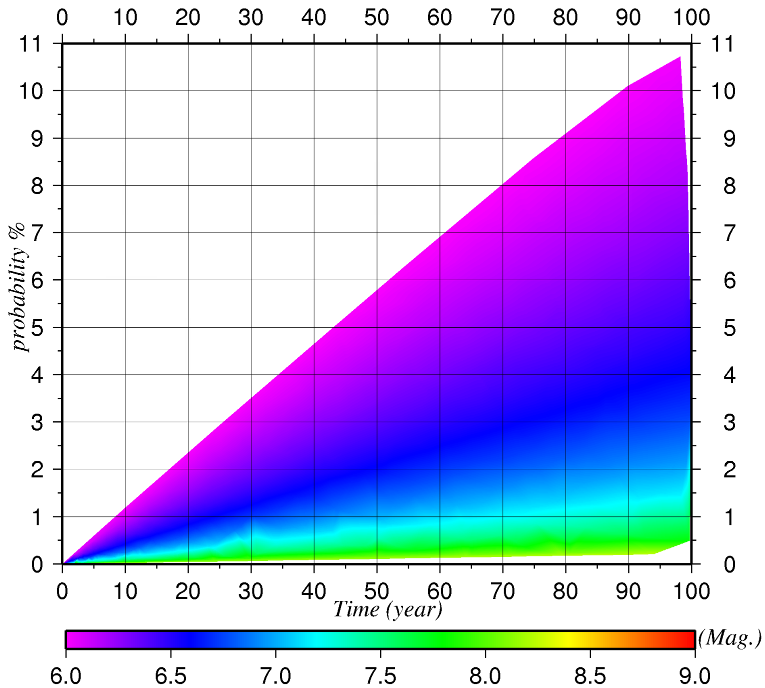

Fig. 7. An example for simulating the magnitude, probability and time of future earthquakes of $M_w \geq 6.0$ for the grid point 120.850° E, 23.850° N.

NHESSD

1, 5729–5752, 2013

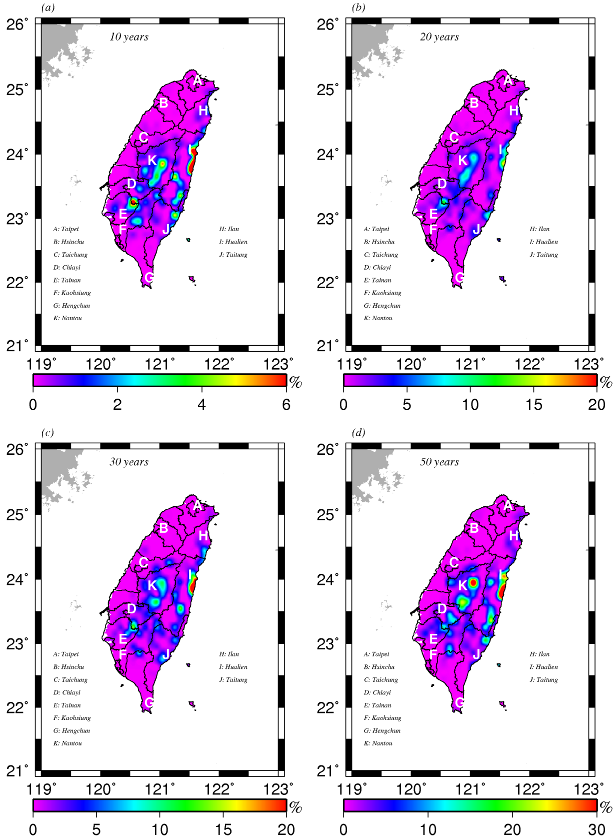

Fig. 8. Simulating probabilities of $M_w \geq 6.0$ earthquakes within the next **(a)** 10, **(b)** 20, **(c)** 30, and **(d)** 50 yr. High probabilities exist from Hsinchu southward to Taichung, Nantou, Chiayi, Tainan and Kaohsiung in western Taiwan and from Ilan southward to Hualian and Taitung in eastern Taiwan.

NHESSD
1, 5729–5752, 2013

Title Page
Abstract | Introduction
Conclusions | References
Tables | Figures
Back | Close
Full Screen / Esc
Printer-friendly Version
Interactive Discussion